



### 저작자표시-비영리-변경금지 2.0 대한민국

이용자는 아래의 조건을 따르는 경우에 한하여 자유롭게

- 이 저작물을 복제, 배포, 전송, 전시, 공연 및 방송할 수 있습니다.

다음과 같은 조건을 따라야 합니다:



저작자표시. 귀하는 원 저작자를 표시하여야 합니다.



비영리. 귀하는 이 저작물을 영리 목적으로 이용할 수 없습니다.



변경금지. 귀하는 이 저작물을 개작, 변형 또는 가공할 수 없습니다.

- 귀하는, 이 저작물의 재이용이나 배포의 경우, 이 저작물에 적용된 이용허락조건을 명확하게 나타내어야 합니다.
- 저작권자로부터 별도의 허가를 받으면 이러한 조건들은 적용되지 않습니다.

저작권법에 따른 이용자의 권리와 책임은 위의 내용에 의하여 영향을 받지 않습니다.

이것은 [이용허락규약\(Legal Code\)](#)을 이해하기 쉽게 요약한 것입니다.

[Disclaimer](#)



공학석사 학위논문

**Evaluation of Non-equal Biaxial Residual  
Stress Using Modified Berkovich  
Indenter in Nano Scale**

나노 스케일에서 Modified Berkovich  
압입자를 활용한 2축 잔류응력 평가

2017년 2월

서울대학교 대학원

재료공학부

XU HUIWEN

# **Abstract**

XU, HUIWEN

Department of Materials Science and Engineering

The Graduate School

Seoul National University

Residual stress is generated by manufacturing processes and thermochemical treatments. These residual stresses combines with external loads to influence deformation and fracture properties. At nanoscale, thin films which have already undergone roll-to-roll processing, have non-equal biaxial residual stress, and this will reduce the reliability of materials. Conventional methods of measuring residual stress, like the x-ray diffraction and curvature methods, have stringent requirements on specimen microstructure or can evaluate only the surface mean residual stress. However, instrumented indentation testing is a non-destructive, simple method that can evaluate local residual stress quantitatively.

On macroscale, the Vickers indenter is used to measure the magnitude of residual stress and the Knoop indenter to evaluate stress directionality. At

nanoscale, the Berkovich indenter is widely used to measure the residual stress magnitude. But no research has been done on evaluating the stress ratio of residual stress using instrumented indentation testing.

In this research, in order to measure biaxial residual stress, a Modified Berkovich indenter was designed that is based on the Berkovich indenter but is extended along one direction to yield different load sensitivity. Before manufacture, we used FEA to verify the validity of this new indenter. Since the Modified Berkovich indenter had geometrical self-similarity, conversion factor ratios were measured for the unstressed and stressed states at a given indentation depth. Moreover, by applying various biaxial stresses to cruciform specimens, the non-equal biaxial residual stress was evaluated by analyzing the load-depth curves. The model was verified by comparing the measured stress with applied stress.

**Keyword:** Instrumented indentation test, Modified Berkovich indenter, Residual stress, Stress ratio, Conversion factor ratio

**Student Number:** 2015-22133

# Contents

<b>Abstract .....</b>	I
<b>Contents .....</b>	III
<b>List of Tables.....</b>	VI
<b>List of Figures .....</b>	VII
<b>Chapter 1. Introduction.....</b>	1
1.1 Objective of the Thesis .....	1
1.2 Outline of the Thesis .....	4
<b>Chapter 2. Research Background .....</b>	7
2.1 About Residual Stress .....	7
2.1.1 Definition of Residual Stress .....	7
2.1.2 Origins of Residual Stress on Nanoscale .....	8
2.2 Measuring Methods of Nano Residual Stress.....	9
2.2.1 X-ray Diffraction Method .....	10
2.2.2 Curvature Method .....	11
2.2.3 Instrumented Indentation Testing .....	12

2.3 Stress Assessment using Indentation Test .....	15
2.3.1 Vickers Indentation Model.....	15
2.3.2. Knoop Indentation Model .....	17
<b>Chapter 3. Modified Berkovich Indenter .....</b>	<b>25</b>
3.1 Limitations of Conventional Indenters .....	25
3.2 Knoop Indenter on Nanoscales .....	27
3.3 New Indenter – Modified Berkovich Indenter.....	29
3.3.1 Design of a New Indenter.....	29
3.3.2 Verification of Modified Berkovich Indenter by FEA.....	31
3.3.3 Checking the Shape of Modified Berkovich Indenter.....	32
<b>Chapter 4. Evaluation of Biaxial Residual Stress using Modified Berkovich Indenter .....</b>	<b>41</b>
4.1 Determination of Conversion Factor Ratio .....	41
4.2 Experimental Details – Conversion Factor Ratio.....	42
4.2.1 Testing Equipment, Specimens and Jig.....	42
4.2.2 Applying Stress.....	43

4.2.3 Experimental Process .....	44
4.3 Evaluation of Biaxial Residual Stress.....	45
4.4 Experimental Details – Biaxial Residual Stress .....	46
4.4.1 Testing Equipment, Specimens and Jig.....	46
4.4.2 Experimental Process .....	47
<b>Chapter 5. Results and Discussion.....</b>	<b>56</b>
5.1 Determination of Conversion Factor Ratio .....	56
5.2 Comparison of Measured Stress Ratio with Applied Stress Ratio .....	57
5.3 Evaluation of Biaxial Residual Stress using Modified Berkovich Indenter and Berkovich Indenter .....	58
<b>Chapter 6. Conclusion.....</b>	<b>68</b>
<b>References.....</b>	<b>69</b>
<b>초 록 .....</b>	<b>69</b>

## **List of Tables**

### **Table 3.1**

Angles of Modified Berkovich indenter

### **Table 4.1**

Materials` mechanical properties and experimental conditions

### **Table 4.2**

Magnitude of applied stresses

### **Table 5.1**

Applied stress ratios and measured stress ratios

### **Table 5.2**

The value of applied stresses and measured stresses

## List of Figures

**Figure 1.1** Effects of residual stress on thin film

**Figure 1.2** Conventional methods of measuring residual stress

**Figure 2.1** Mechanisms of thermal stress, intrinsic stress and epitaxial stress

**Figure 2.2** The schematic draws of X-ray diffraction method

**Figure 2.3** The schematic draws of curvature method

**Figure 2.4** Indentation load-depth curve

**Figure 2.5** Illustration of residual stress effect on indentation depth under the same load

**Figure 2.6** The schematic draw of indentation load-depth curve under unstressed and stressed states

**Figure 3.1** Conventional indenters for measuring residuals stress

**Figure 3.2** OM image of Knoop tip angle

**Figure 3.3** SEM image of Knoop sharp point

**Figure 3.4** Schematic diagram of Knoop indenter offset

**Figure 3.5** Schematic diagram of geometrical self-similarity

**Figure 3.6** Schematic diagram of Modified Berkovich indentation and Berkovich indentation

**Figure 3.7** The position of indenter tip point

**Figure 3.8** Angles between centerline and two faces

**Figure 3.9** Finite element analysis modeling of Modified Berkovich indenter

**Figure 3.10** Load-depth curve from indentation test by FEA

**Figure 3.11** OM image of tip angle of Modified Berkovich indenter

**Figure 3.12** SEM image of sharp point of Modified Berkovich indenter

**Figure 4.1** Definitions of conversion factors

**Figure 4.2** Four-point bending jig

**Figure 4.3** Example of stress distribution of bending specimen

**Figure 4.4** Modified Berkovich indenter made by PROBES

**Figure 4.5** Nano AIS made by Frontics Inc., Korea

**Figure 4.6** Nano indentation machine made by Anton Paar

**Figure 4.7** Load-depth curves from different direction of indentations

**Figure 4.8** Biaxial stress applied jig and cruciform

**Figure 5.1** Results of conversion factor ratios at different indentation depth(1)

**Figure 5.2** Results of conversion factor ratios at different indentation depth(2)

**Figure 5.3** Results of conversion factor ratios at different indentation depth(3)

**Figure 5.4** Results of conversion factor ratios at different indentation depth(4)

**Figure 5.5** Conversion factor ratios at various indentation depth

**Figure 5.6** Results of measured stress ratio and applied stress ratio

**Figure 5.7** Comparison of applied stress and measured stress

# **Chapter 1. Introduction**

## **1.1 Objective of the Thesis**

Residual stress is defined as the stress state in materials in the absence of any external load [1]. Materials generate residual stresses during manufacturing processes such as rolling, bending, forging, and pressing, and during thermochemical treatments. These residual stresses and external stresses influence materials` deformation and fracture properties. It is very important to evaluate residual stress because it can decrease not only tensile properties like yield strength but also the fatigue strength and fracture properties of structures. At micro/nanoscale, especially in the thin film industry, evaluation of residual stress is important to prevent failures such as bending, twisting, buckling and cracking, as shown in Fig. 1.1.

The most common methods of measuring residual stress in nanoscale are the x-ray diffraction method and curvature method (Fig. 1.2). Since both these methods are non-destructive, they do not generate plastic deformation in the specimen for stress relaxation. However, when using the x-ray diffraction method to measure residual stress, the results can be easily influenced by the material`s microstructure. In addition, the curvature

method cannot evaluate the local residual stress.

Instrumented indentation testing (IIT), which is a form of hardness testing, is considered as a replacement for the conventional methods. The differences between IIT and a conventional hardness test are that IIT senses the load and indentation depth in real time and that is not necessary to measure the indentation area.

Many studies have sought to evaluate residual stress with IIT. Suresh and Giannakopoulos [2] proposed a theoretical model using a sharp indenter to evaluate the equibiaxial stress. They used the ratio of true contact area of stressed and unstressed samples to set up a model.

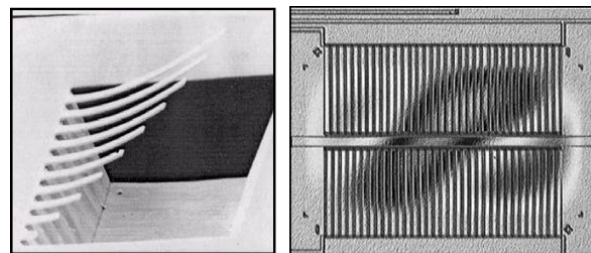
Lee and Kwon [3,4] formulated a modified sharp indentation model that picks up the plastic-deformation-interactive deviatoric stress component from residual stress.. The limitation of the model is that it is possible to evaluate the non-equibiaxial residual stress.

Han's model [5] used a Knoop indenter to overcome the limitation. The Knoop indenter, which has the ratio of long and short diagonal of indenter as 7.11:1 with two-fold symmetry, is used to assess material anisotropy due to directional hardness [7-22]. Han's model was set up in terms of the load difference of two Knoop indentations at two orthogonal axes along the principal directions. The ratio of conversion factors that are proportional

constants normal and parallel to the uniaxial residual stress with a Knoop indenter is experimentally taken as 0.34.

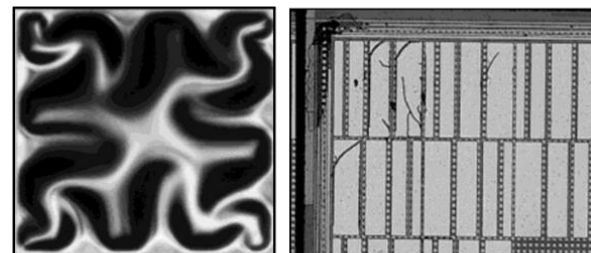
## **1.2 Outline of the Thesis**

This thesis has six chapters. The objective and outline of the research are introduced in chapter 1. Chapter 2 discusses the meaning, origins, and measuring methods for residual stress, and also briefly introduces basic principles of instrumented indentation testing and the evaluation of residual stress using instrumented indentation. Chapter 3 first, introduces the limitations of the Knoop indenter at nanoscale and then discusses issues and approaches about design of Modified Berkovich indenter. The theoretical Modified Berkovich indenter model and experimental details such as testing machine, specimens, jigs and experiment processes are introduced in chapter 4. Chapter 5 describes experiment results and discussion. Chapter 6 summarizes the research.



Bending

Twisting



Buckling

Cracking

**Figure 1.1** Effects of residual stress on thin film

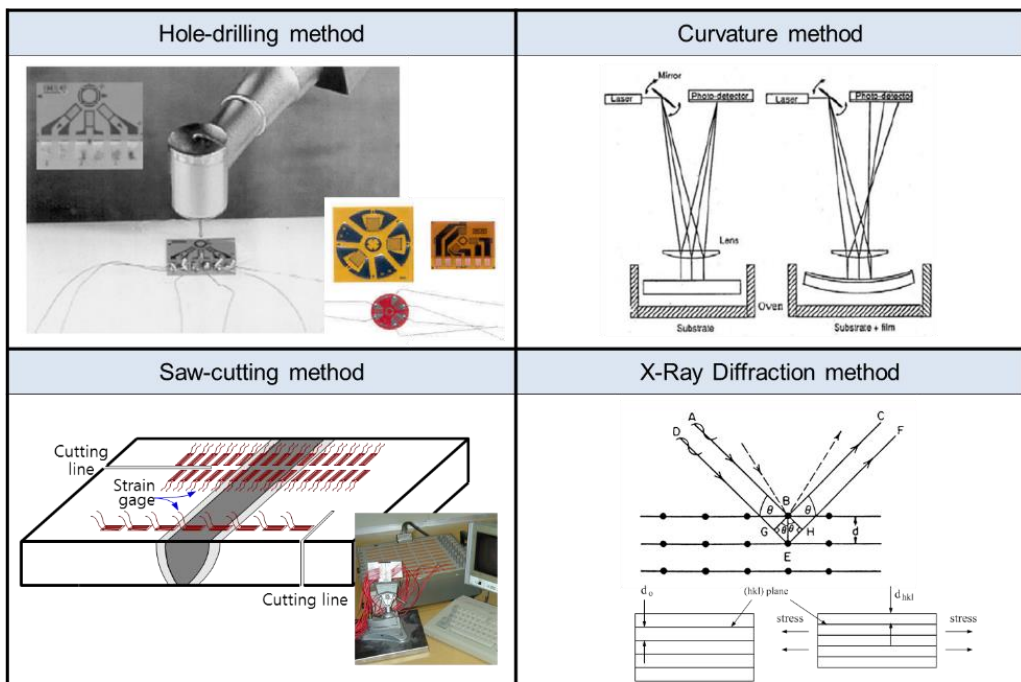


**Figure 1.2** Conventional methods of measuring residual stress

## **Chapter 2. Research Background**

### **2.1 About Residual Stress**

#### **2.1.1 Definition of Residual Stress**

Residual stress is defined as stress state which exists within materials in the absence of any external load [1]. Residual stress can be divided into macro residual stress and micro/nano residual stress. Discontinuous plastic deformation may be induced during mechanical processing and thermal treatments such as welding, rolling, thin film processing, and quenching, and can finally result in macro residual stress. Micro/nano residual stress, on the other hand, is usually caused by different mechanical properties of phases, atomic mismatch, and dislocations. Excessive residual stress lessens material lifetime, and may ultimately cause unexpected fracture.

### **2.1.2 Origins of Residual Stress on Nanoscale**

Residual stress in thin films usually occurs during vacuum deposition and is conventionally classified into three types: thermal stress, intrinsic stress and epitaxial stress (Fig. 2.1) [24-26]. Thermal stress occurs due to thermal mismatch caused by different thermal expansion coefficients of the thin film and substrate. When a metal thin film is deposited on a silicon substrate at high temperature, the thermal expansion coefficient of the thin film is generally higher than that of the substrate. Epitaxial stress is produced by the tendency to keep the coherency of film and substrate of similar atomic constants. Intrinsic stress is defined as a self-generated stress during film growth. Microstructural changes such as grain boundaries, dislocations, vacancies, impurities, and secondary phases or phase transformations cause changes in density, and elastic strain and stress are induced to maintain coherency between substrate and volume.

## **2.2 Measuring Methods of Nano Residual Stress**

Residual stress has considerable effects on material strength, fatigue and fracture. For examples, tensile stress induces cracking in thin films and severe compressive stress separates a thin film from its substrate. Also, in addition, the plastic deformation caused by residual stress has a detrimental influence on product reliability. Hence the evaluation of residual stress is necessary.

### 2.2.1 X-ray Diffraction Method

The x-ray diffraction method evaluates residual stress by assessing lattice spacing by measuring the diffraction angle (Fig. 2.2). When x-rays pass through metal surface, the crystal plane that accords with Bragg conditions has a diffraction peak. If residual stress is present, the lattice spacing will contract and release, which may change the width and occurrence position of the diffraction peak. The residual stress  $\sigma_\phi$  can be calculated from:

$$\frac{d_{\psi,\phi} - d_0}{d_0} = \frac{1}{E} [\sigma_\phi (1 + \nu) \sin^2 \psi] \quad (2-1)$$

Here,  $d_{\psi,\phi}$  and  $d_0$  are the lattice spacing of the stressed state and stress free state -  $E$  is the elastic modulus,  $\nu$  is Poisson's ratio, and  $\psi$  is the reflection angle.

Although the x-ray diffraction method can measure residual stress nondestructively, the method has the limitation that the specimen must have regular crystalline structure, since the result can easily be affected by microstructural factors.

## 2.2.2 Curvature Method

The curvature method is mostly used to evaluate residual stress in thin films. The method evaluates residual stress by measuring the curvature of the substrate using laser scanning, optical interferometry and so on (Fig. 2.3). Residual stress can be easily calculated from the Stoney equation:

$$\sigma_f = \left( \frac{E}{1-\nu} \right)_s \frac{t_s^2}{6t_f} \frac{1}{R_{curv}} \quad (2-2)$$

where  $t_s$  and  $t_f$  are the thickness of substrate and thin film and  $R_{curv}$  is the measured curvature radius of the thin film.

### **2.2.3 Instrumented Indentation Testing**

The instrumented indentation test is a non-destructive method to evaluate materials` mechanical properties and stress state. IIT has been developed from conventional hardness testing; it is simple to perform and does not require any particular specimen dimensions. The advantage of IIT is that it can sense the load and displacement in real time during the test (Fig. 2.4). IIT not only measures elastic modulus, hardness, strength but also evaluates residual stress and adhesion. IIT theory has advanced to assessing biaxial residual stress on macroscale.

When material is under compressive stress, it can be considered to have been squeezed, so that under a given load, it is harder to penetrate than in the stress-free state. Similarly, when a material is under tensile stress, it is easier to penetrate at a given load than in the stress-free state (Fig. 2.5). When a material is under residual stress, its indentation load-depth curve shifts by the magnitude and direction of residual stress. Hardness and elastic modulus are invariant whether or not residual stress exists in a material.

Previous research on using instrumented indentation test to evaluate residual stress exploits the relationship between hardness difference and applied stress. Sines and Carlson [27] measured the difference in Rockwell

hardness on artificially strained metallic materials to give assess their residual stress state. Frankel [28] tried to establish a model by analyzing the quantitative effect of residual stress on indentation yielding by stress-sensitive behavior related to Rockwell hardness. But the limitation of the method is that some experimental constants and yield strength must be known before it can be applied.

Research on evaluating residual stress using indentation testing soon expanded to nanoscales, especially thin films. Tsui et al. [29], studied the effect of in-plane stress on indentation plasticity using the load-depth curve and contact area. They reported that the contact hardness remained constant regardless of elastically applied stress. This invariant hardness came to be a significant assumption in subsequent studies on finite element analysis.

Suresh and Giannakopoulos [2] suggested a model to evaluate equibiaxial thin-film stress using a sharp indenter. They took the equibiaxial thin-film stress as the sum of hydrostatic stress and differential contact stress and found that the difference in contact area of stressed and unstressed materials at the same indentation depth was related to the residual stress.

Lee and Kwon [4] studied a method for quantitative evaluation of the biaxial stress state. They extract the deviatoric stress component from sum of the non-equibiaxial residual stress. As a three-dimensional elastic stress,

hydrostatic stress does not influence plastic deformation and indentation load. However, z-directional deviatoric stress, which has the same directional component as the loading direction, can affect the indentation load. The method used the relation between indentation load difference and residual stress.

## 2.3 Stress Assessment using Indentation Test

### 2.3.1 Vickers Indentation Model

The key point in evaluating residual stress is the load difference in the unstressed and stressed states. When materials have tensile or compressive residual stress, the load-depth curve getting from indentation test shifts from that in the unstressed state (Fig. 2.6). Suresh and Giannakopoulos [2] built a model of equibiaxial residual stress, assuming that material hardness is constant and that, when the penetrating depth is equal the change in indentation load reflects the residual stress. The change in indentation load was defined as the differential contact load. Because equibiaxial stress was regarded as subtracting a uniaxial stress from a hydrostatic stress, the differential contact load in the unstressed and stressed state was expressed as the residual stress and contact area.

Since the method contained hydrostatic components and because it was difficult to measure the residual stress, Lee and Kwon [4] suggested a new method to evaluate equibiaxial residual stress by linking  $L_{res}$  to  $-(1+p)\sigma_{res}/3$  from the deviatoric stress component. The mathematical tensor form of this method is given as:

$$\begin{array}{c}
 \text{Biaxial stress} \\
 \overbrace{\left( \begin{array}{ccc} \sigma_{res,x} & 0 & 0 \\ 0 & \sigma_{res,y} & 0 \\ 0 & 0 & 0 \end{array} \right)}^{\text{Hydrostatic stress}} = \overbrace{\left( \begin{array}{ccc} \sigma_{res,x} & 0 & 0 \\ 0 & p\sigma_{res,x} & 0 \\ 0 & 0 & 0 \end{array} \right)}^{\text{Deviatoric stress}} = \\
 \left( \begin{array}{ccc} \frac{(1+p)}{3}\sigma_{res,x} & 0 & 0 \\ 0 & \frac{(1+p)}{3}\sigma_{res,x} & 0 \\ 0 & 0 & \frac{(1+p)}{3}\sigma_{res,x} \end{array} \right) + \left( \begin{array}{ccc} \frac{(2-p)}{3}\sigma_{res,x} & 0 & 0 \\ 0 & \frac{(2-p)}{3}\sigma_{res,x} & 0 \\ 0 & 0 & -\frac{(1+p)}{3}\sigma_{res,x} \end{array} \right)
 \end{array} \quad (2-3)$$

If the directionality  $p$  is known, the residual stress at the  $x$ -axis and  $y$ -axis is given as:

$$\begin{aligned}
 \sigma_{res,x} &= \frac{3\Delta L}{(1+p)A_c^T} \\
 \sigma_{res,y} &= p\sigma_{res,x} = \frac{3p\Delta L}{(1+p)A_c}
 \end{aligned} \quad (2-4)$$

### 2.3.2. Knoop Indentation Model

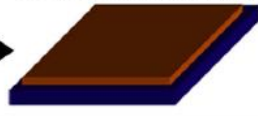
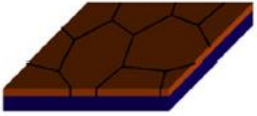
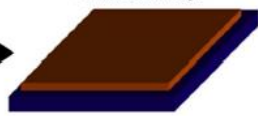
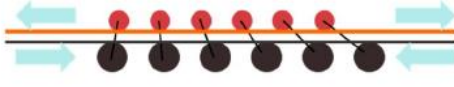
When a specimen is under non-equal biaxial stress state, the indentation load-depth curve shifts from unstressed state, and the change in load depends on the orientation of the Knoop indenter. It is assumed that the residual stress and load difference has a linear relationship at a fixed indentation depth. Since the ratio of the long and short diagonals of Knoop indenter is 7.11:1, at a fixed indentation depth, the load difference is made by Knoop indenter according to the direction of the long axis. When a material has non-equal biaxial residual stress the relation between the load difference and residual stress is given as:

$$\begin{aligned}\Delta L_1 &= \alpha_{\perp} \sigma_{res}^x + \alpha_{//} \sigma_{res}^y \\ \Delta L_2 &= \alpha_{//} \sigma_{res}^x + \alpha_{\perp} \sigma_{res}^y\end{aligned}\quad (2-5)$$

where  $\alpha_{\perp}$  and  $\alpha_{//}$  are conversion factors and  $\Delta L_1$ ,  $\Delta L_2$  are the load at a fixed depth in the unstressed state and stressed state. Han et al. [5] showed that the relationship between conversion factor ratio and load difference ratio is

$$\frac{\Delta L_2}{\Delta L_1} = \frac{\frac{\alpha_{//}}{\alpha_{\perp}} + \frac{\sigma_{res}^y}{\sigma_{res}^x}}{1 + \frac{\alpha_{//}}{\alpha_{\perp}} \frac{\sigma_{res}^y}{\sigma_{res}^x}} = \frac{\frac{\alpha_{//}}{\alpha_{\perp}} + p}{1 + \frac{\alpha_{//}}{\alpha_{\perp}} p} \quad (2-6)$$

where  $\alpha_{\parallel}/\alpha_{\perp}$  is a conversion factor ratio that was derived experimentally and taken as 0.34 on macroscale. In order to estimate  $p$  in Eq. 2-6, the conversion factor ratio must be known, and the load difference  $\Delta L_1$ ,  $\Delta L_2$  should be derived from experiment. Using a Vickers indenter, we can evaluate the sum of perpendicular and parallel residual stresses to the principal direction, and the stress ratio can be obtained by using Knoop indenter. In the end, we can evaluate the quantitative residual stresses  $\sigma_{res}^x$  and  $\sigma_{res}^y$  respectively.

	Cause	Mechanism
<b>Thermal stress</b>	<b>Adhesion</b> (Maintenance of adhesion)	At high temperature : stress relaxation  → Cooling down : volume shrinkage induced by coefficient of thermal expansion 
<b>Intrinsic stress</b> (growth stress)		Polycrystalline structure  → Grain growth and volume shrinkage 
<b>Epitaxial stress</b>	<b>Coherency</b> (Relief of atomic mismatch, maintenance of coherency)	

**Figure 2.1** Mechanisms of thermal stress, intrinsic stress and epitaxial stress

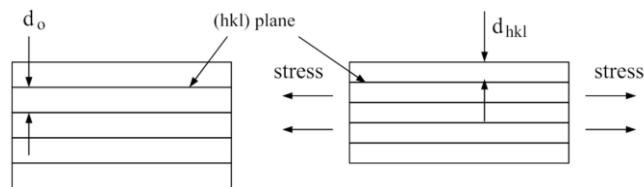
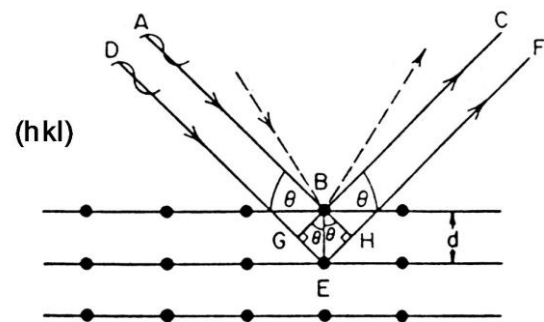


**Figure 2.2** The schematic draws of X-ray diffraction method

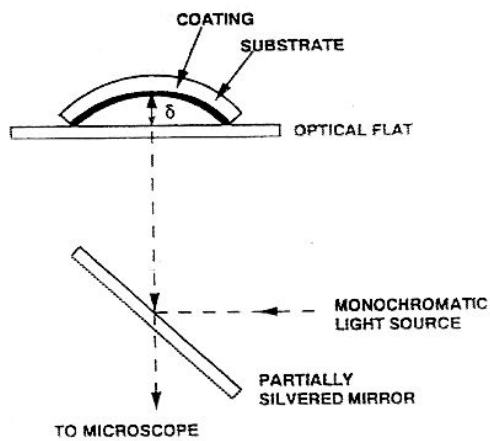
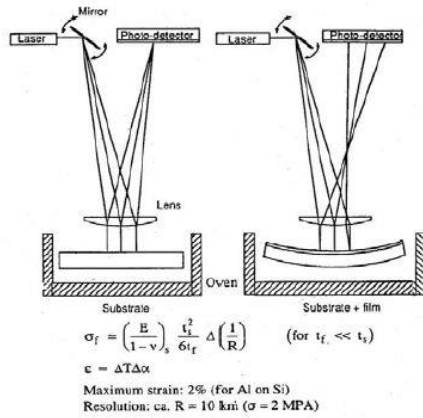


**Figure 2.3** The schematic draws of curvature method

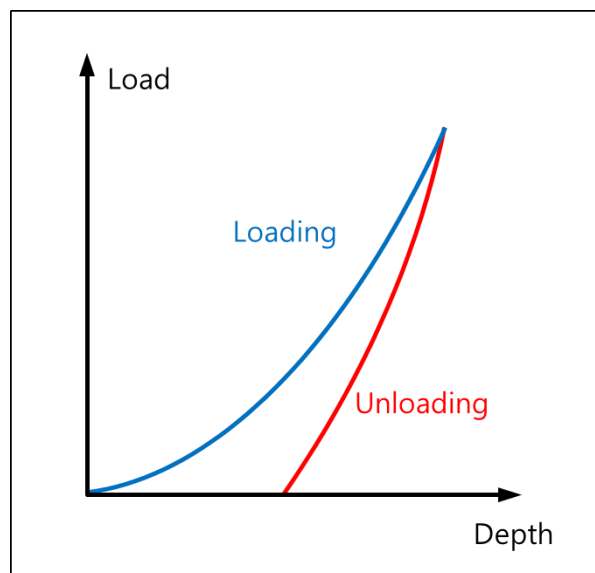


**Figure 2.4** Indentation load-depth curve

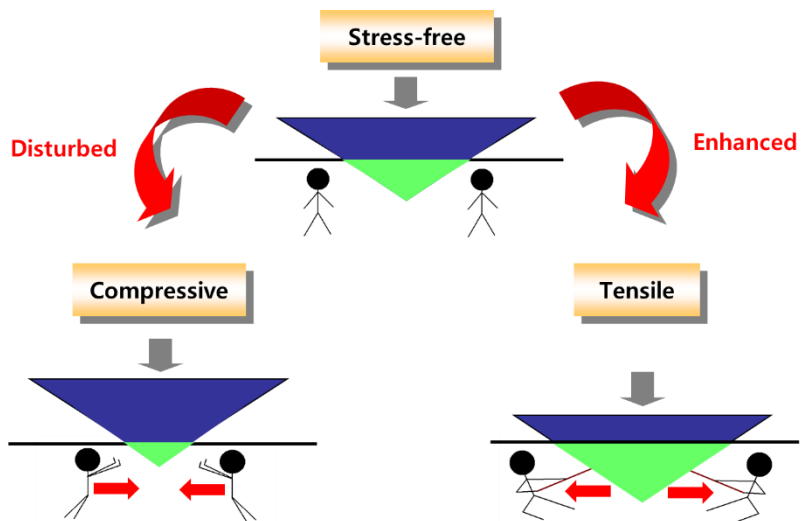


**Figure 2.5** Illustration of residual stress effect on indentation depth under the same load

Indentation load-depth curve

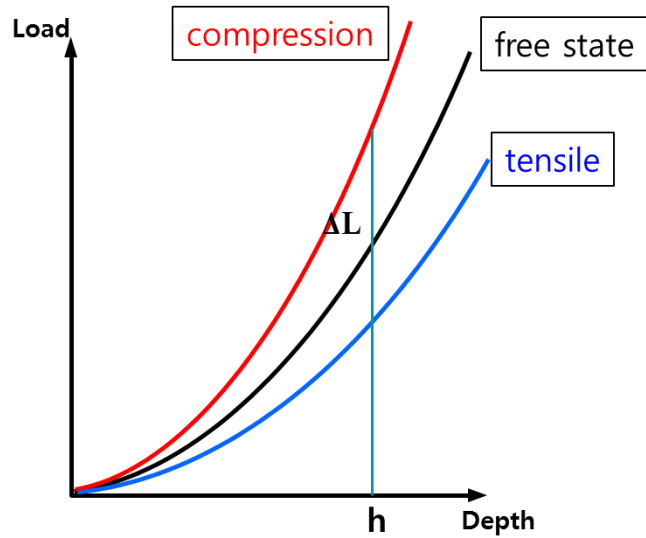


**Figure 2.6** The schematic draw of indentation load-depth curve under unstressed and stressed states

## **Chapter 3. Modified Berkovich Indenter**

### **3.1 Limitations of Conventional Indenters**

Over the last few years, evaluation of residual stress using instrumented indentation technique has become more and more popular, since it is easy to do experiments and get quantitative value for residual stress from the real-time load-depth curve. Conventional indenters like the Vickers, Knoop, and Berkovich indenters are used to measure residual stress (Fig. 3.1). Specifically, on macroscale, the Vickers indenter is used to evaluate the sum of the *x-axis* residual stress and *y-axis* residual stress, known as the magnitude of residual stress. However, on microscale or nanoscale, the Berkovich indenter is chosen to appraise the magnitude of residual stress. The reason that the Vickers indenter and Berkovich indenter are used in the different cases is because Vickers indenter is a pyramid indenter with four triangular faces which join at a common point. However, at micro or nano sizes, it is difficult to make the four side faces of Vickers indenter to come together at one tip point. The Berkovich indenter is, on the other hand, easier to make since the tip of Berkovich indenter has of only three faces at a point.

The Knoop indenter is usually used to measure the stress ratio of residual

stress on macroscale. The Knoop indenter, with four-fold symmetry indenter, has different diagonal lengths, which means that the load sensitivity measured by indentation testing will differ according to the direction of the indenter. We thus face the problem of which indenter to use to evaluate the stress ratio of residual stress on nanoscale. There are two possible strategies: first, proportionally decrease the size of the Knoop indenter to nanoscale. Or second, customize a new indenter.

## 3.2 Knoop Indenter on Nanoscales

At first, we adopted the first strategy – manufacturing a Knoop indenter on nanoscale. OM (optical microscopes) image of the Knoop tip angle shows that a nanoscale Knoop indenter has good agreement with the angle specification (Fig. 3.2). However, from SEM (scanning electron microscope) image of a Knoop tip point (Fig. 3.3), we found that four side faces of Knoop indenter joined not at one tip point, but at two points. The line of junction between opposite faces is called indenter offset and is defined in ASTM standard E384-16. From this ASTM standard, if the indentation length is 20  $\mu\text{m}$ , the offset should not be greater than over 1.0  $\mu\text{m}$ . For shorter indentation lengths, the offset should be proportionately less than 1.0  $\mu\text{m}$  (Fig. 3.4). The offset of the Knoop indenter as gauged by SEM is 0.592  $\mu\text{m}$ . The ratio of offset and indentation length should be less than 1.0  $\mu\text{m} : 20 \mu\text{m}$ . In this case, since offset of Knoop indenter is 0.592  $\mu\text{m}$ , indentation length must be greater than 11.84  $\mu\text{m}$ . Then, through the geometry of the Knoop indenter, we can easily calculate that the penetration depth must be more than 689 nm. For example, when the indenter penetrates 1000nm, the indentation length is 17.189  $\mu\text{m}$  and the ratio of offset and indentation length is 0.034. However, if the indenter penetrates 400 nm , the indentation

length is  $6.88 \mu\text{m}$  and the ratio of offset and indentation length will be 0.086, greater than the required value of 0.05. In this research, we consider indentation depth from 200 nm to 1000 nm, so it is clear that the offset of the Knoop indenter does not meet the requirements of the ASTM standard.

### **3.3 New Indenter – Modified Berkovich Indenter**

#### **3.3.1 Design of a New Indenter**

Since the Knoop indenter does not accord with the standard, we decided to customize a new indenter. One of the most important steps in making a new indenter is how to design. There are three issues to be considered. First of all, the conversion factor ratio, which is a significant parameter for measuring the stress ratio of residual stress, is constant regardless of indentation depth. Second, in penetrating two orthogonal indentations at the same stress state, their load sensitivity should be different. Last but not least, the stability of indenter and equipment during indentation testing must be considered.

In order to satisfy those issues, we used the following approaches in designing the new indenter. To keep the conversion factor ratio constant, the indenter should have geometrical self-similarity (Fig. 3.5). Also, to achieve different load sensitivity, the indenter should be two-fold rotationally symmetric or mirror symmetric. So we designed the new indenter based on the Berkovich indenter, which has geometrical self-similarity, and extended the Berkovich indenter three times along one direction to sense load, as shown in Fig. 3.6. As we know, the Berkovich indenter has four tip points; three of them are already determined and where to put the fourth point is

very important. Only by setting the indenter tip point on the center of gravity could we ensure the accuracy of indentation data, since if the indenter tip point deviates from center of gravity, like first and third triangles in Fig. 3.7, three triangles will suffer different stresses. Finally, we designed a new indenter that we call the Modified Berkovich indenter. The angles of centerline and indenter faces are  $65.3^\circ$  and  $80.1^\circ$  (Fig. 3.8).

### **3.3.2 Verification of Modified Berkovich Indenter by FEA**

Before manufacturing the Modified Berkovich indenter, in order to verify its validity, we used finite element analysis (FEA) to simulate indentation testing. First, we simulated indentation test on a material surface in the unstressed state. Then uniaxial tensile stress was applied to a specimen, and we simulated indentation testing twice to make the direction of indentations orthogonal. We got three indentation load-depth curves from these simulations. The result shows (Fig. 3.10) that the load difference is 0.64 mN in the parallel direction; and 1.522 mN in the vertical direction. It is clear that in the same stress state, the load difference varies according to the direction of symmetry axis of Modified Berkovich indenter.

### **3.3.3 Checking the Shape of Modified Berkovich Indenter**

The Modified Berkovich indenter was made of diamond by PROBES.

From the OM image of tip angle (Fig. 3.11) and SEM image of sharp point (Fig. 3.12), we can see that Modified Berkovich indenter was made as expected. The errors in indenter angles are less than  $0.5^\circ$  (Table 3.1).

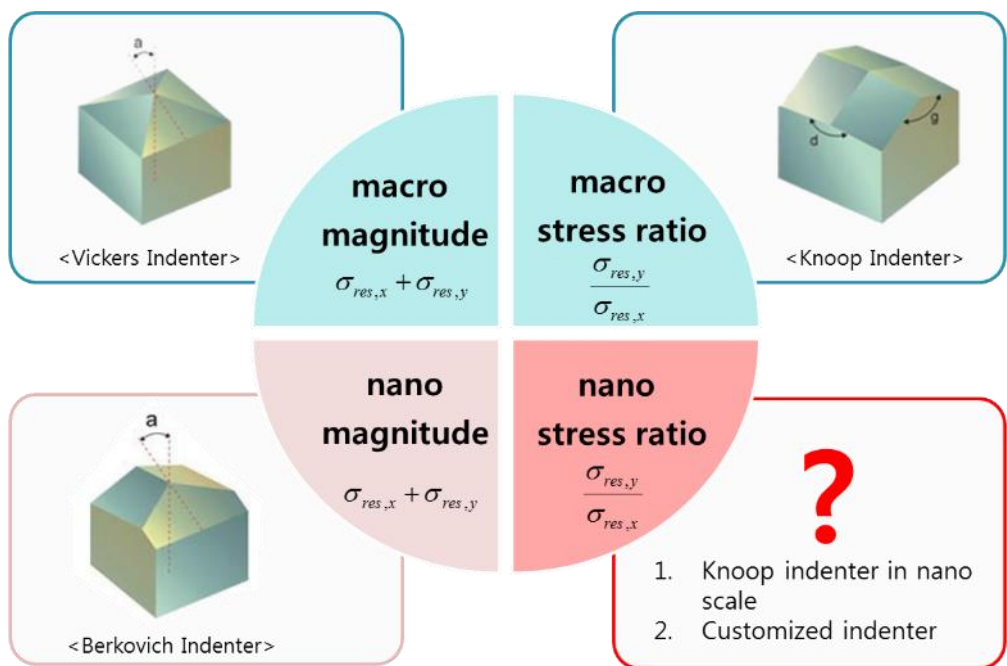


**Figure 3.1** Conventional indenters for measuring residuals stress

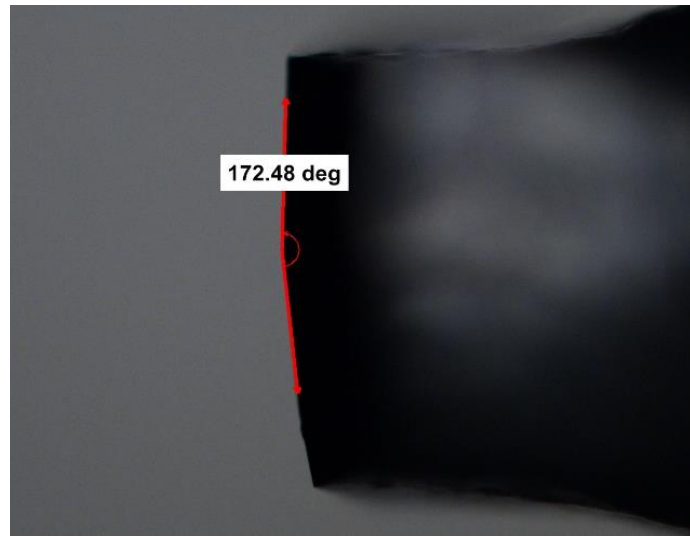


**Figure 3.2** OM image of Knoop tip angle

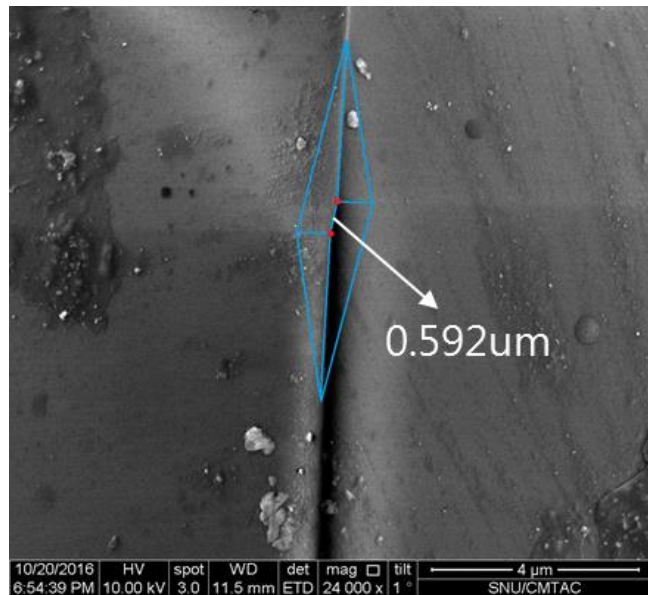


**Figure 3.3** SEM image of Knoop sharp point

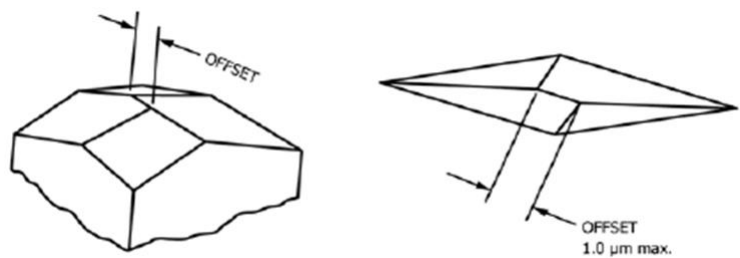


**Figure 3.4** Schematic diagram of Knoop indenter offset

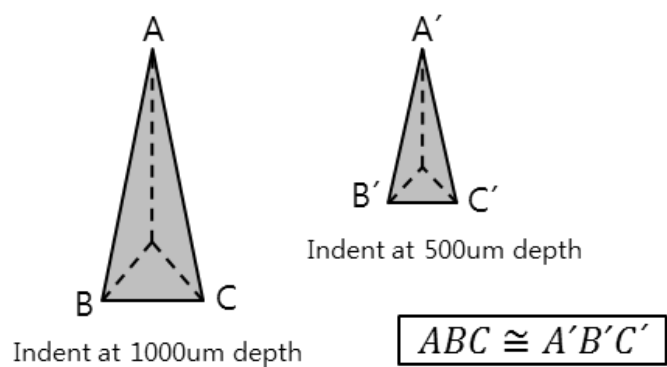


**Figure 3.5** Schematic diagram of geometrical self-similarity

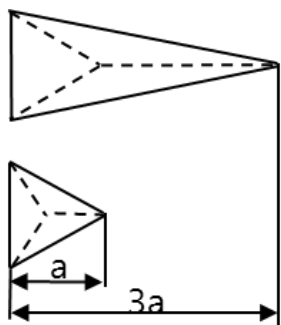
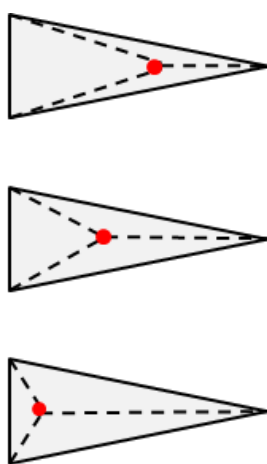


**Figure 3.6** Schematic diagram of Modified Berkovich indentation and Berkovich indentation



the position of tip point  
(red point)

**Figure 3.7** The position of indenter tip point

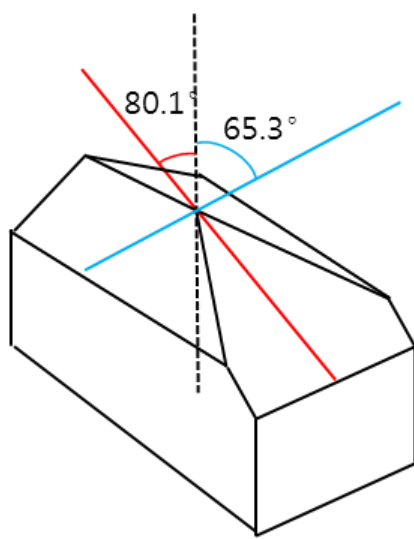


**Figure 3.8** Angles between centerline and two faces

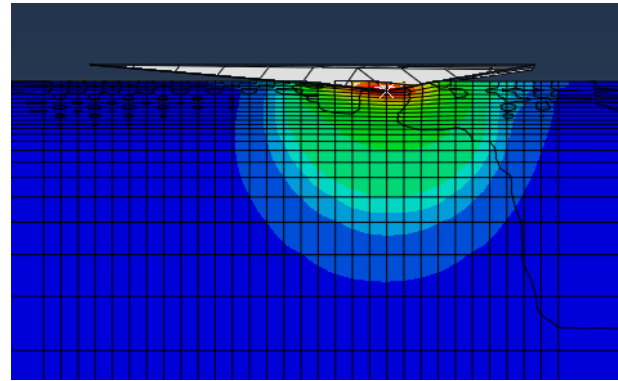


**Figure 3.9** Finite element analysis modeling of Modified Berkovich indenter

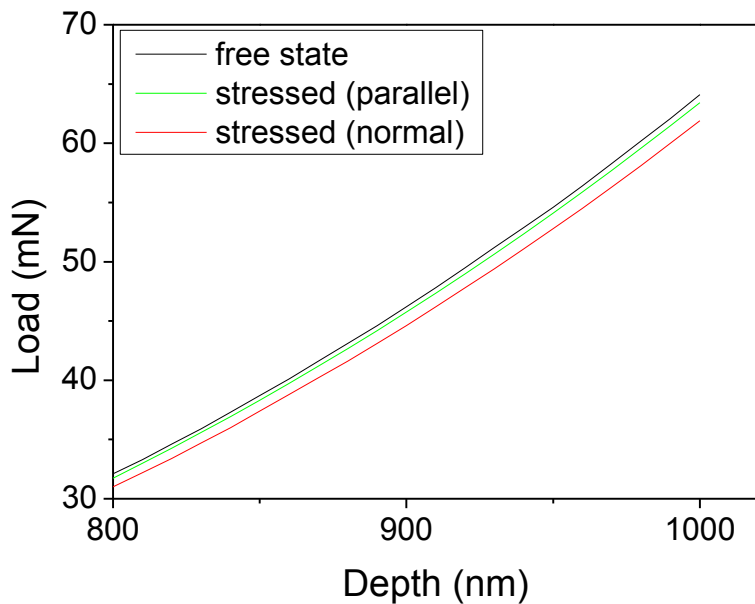


**Figure 3.10** Load-depth curve from indentation test by FEA

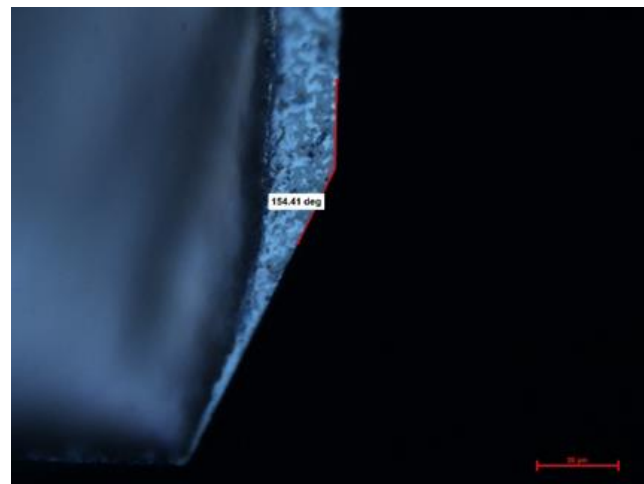


**Figure 3.11** OM image of tip angle of Modified Berkovich indenter

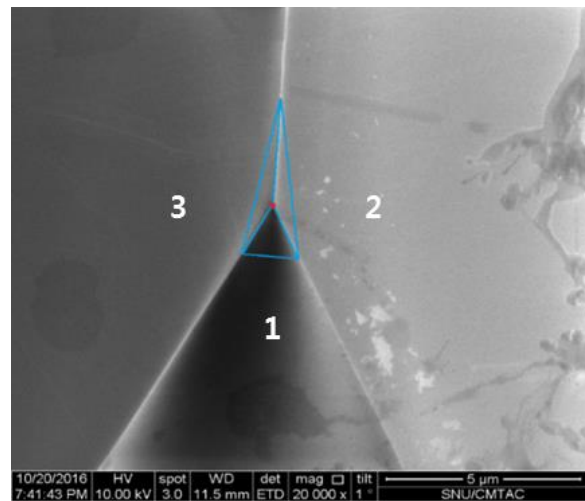


**Figure 3.12** SEM image of sharp point of Modified Berkovich indenter

angles	nominal	measured
$a_1$	80.10	80.03
$a_2$	65.30	65.42
$a_3$	65.30	65.45
$b_{12}$	100.90	100.68
$b_{13}$	259.10	259.25

**Table 3.1** Angles of Modified Berkovich indenter

## **Chapter 4. Evaluation of Biaxial Residual Stress using Modified Berkovich Indenter**

### **4.1 Determination of Conversion Factor Ratio**

On the macroscale, in order to evaluate biaxial residual stress, Han et al.[5] and Choi et al.[23] suggested conversion factors to link the load difference and residual stress (Fig. 4.1). They found that conversion factor ratio is constant at 0.34 regardless of material, residual stress state and indentation depth. Each type of indenters has their own conversion factor ratios. We decided to adopt the macro conversion factor ratio model to nanoscale. As we know, the conversion factor is defined as the ratio of the load difference to stress when the material under uniaxial stress.

$$\begin{aligned}\Delta L_{\perp} &\approx \alpha_{\perp} \sigma_{res}^x \\ \Delta L_{//} &\approx \alpha_{//} \sigma_{res}^x\end{aligned}\quad (4-1)$$

Here,  $\sigma_{res}^x$  is residual stress along  $x$ -axis.  $\Delta L_{\perp}$ ,  $\Delta L_{//}$  are load differences between the unstressed state and residually stressed state at a certain depth, and  $\alpha_{\perp}$  and  $\alpha_{//}$  are the nominal conversion factor and parallel conversion factor, respectively. We distinguish two kinds of conversion factor according to the direction of the symmetry axis of the indentation.

## **4.2 Experimental Details – Conversion Factor Ratio**

### **4.2.1 Testing Equipment, Specimens and Jig**

The Modified Berkovich tip made of diamond by Probes Inc. (Fig. 4.4), is used for instrumented indentation test. In our experiments, we used two different pieces of equipment to do for indentation tests. One is NANO AIS made by Frontics Inc., Republic of Korea (Fig. 4.5). The resolution of load and displacement are 10 nN and 0.04 nm, and the maximum load is 200 mN. The other is Ultra Nano Indentation made by Anton Paar, Switzerland (Fig. 4.6). The resolution of load and displacement are 1 nN and 0.03 nm, and the maximum load is 100 mN. All experiments were done under displacement control.

In order to determine the conversion factor ratio, we prepared five kinds of materials: CuC1100, Al6061, SUS316, SUS304, and S45C. Their mechanical properties such as elastic modulus and yield strength are shown in Table 4.1. All specimens were annealed to release residual stress. Indentation samples were finely polished with diamond suspension 0.25  $\mu\text{m}$ . In order to induce residual stress easily and conveniently, a four-point bending jig was used to apply stress (Fig. 4.2).

#### **4.2.2 Applying Stress**

Before inducing stresses using the four-point bending jig, we must polish the faces of the specimen and then attach 3 mm strain gauge to the specimen surface. We use  $120\ \Omega$  strain gauges made by Showa Measuring Instruments Co., Ltd, Japan. When we adjusted screws, the indicator sensed change in strain, so that we knew the stress applied to the specimen in real time. Fig. 4.3 shows applied stress state of bending specimen, where two sides have opposite stresses. It is assumed that when one side has 360 MPa tensile stress, the other side has 360 MPa compressive stress. Along a line which is parallel to the dotted line, stresses are applied uniformly despite of indentation depth. The real values of the applied stresses are shown in Table 4.1.

### **4.2.3 Experimental Process**

Before inducing stress, we did the following experiment in order to get the stress-free indentation load-depth curve. After polishing the surface of sample, we did indentation tests in the unstressed state. Each material has predetermined indentation depths, as shown in Table 4.1. At a fixed indentation depth, we repeated indentation testing three times. In order to be unaffected by the adjoining indent's plastic zone, the distance between two indentations is  $50 \text{ nm} \sim 70 \text{ nm}$ , which is the plastic zone size. Then we attached strain gauges to the surface of specimen, and read the real-time value of applied stress through the change of strain. It is assumed that if the applied stress is oriented along the  $x$ -axis, we repeated indentation tests, in which the long diagonal is oriented along  $x$ -axis and  $y$ -axis. Finally, we derive the load difference  $\Delta L_1$ ,  $\Delta L_2$  at maximum depth from the indentation load-depth curves (Fig. 4.7).

### 4.3 Evaluation of Biaxial Residual Stress

We now evaluate the stress ratio in biaxial residual stress. When a material is in a biaxial residual stress state, we can consider the load difference between the stress-free state and biaxial stressed state as the algebraic sum of two load differences from the stress-free and uniaxial stressed states. The conversion factor ratio is independent of material and indentation depth. To calculate stress ratio  $p$  in Eq. 2-6, we need the load difference ratio from indentation test using the Modified Berkovich indenter.

To evaluate the surface residual stress by instrumented indentation testing with a Berkovich indenter and Modified Berkovich indenter, the load difference between the stressed state and stress-free state is needed. A novel modeling with Modified Berkovich indenter is introduced. The biaxial residual stress is found using by Eq. 2-4 and Eq. 2-6.

## **4.4 Experimental Details – Biaxial Residual Stress**

### **4.4.1 Testing Equipment, Specimens and Jig**

The indenter and testing equipment are as same as those used in determining the conversion factor ratio. In this experiment, we want to evaluate the stress ratio, which means specimen must be in a biaxial stressed state. So instead of bending jig, we chose biaxial stress applied jig and cruciform specimen. The specification of jig and specimen are shown in Fig. 4.8. All samples went through stress relaxation by annealing and the surfaces were finely polished with diamond suspension  $0.25 \mu\text{m}$ .

#### **4.4.2 Experimental Process**

Five materials, CuC1100, Al6061, SUS316, SUS304, S45C, were used in evaluating the stress ratio of biaxial residual stress. This time, however, the indentation depth was fixed at 1000  $\mu\text{m}$ .

First, we do indentation tests in the stress-free state. Here, again, we repeat each test three times, and the distance between two indentations is held at 70 nm. Then stresses were induced in the specimen of the magnitudes shown in Table 4.2. Indentation testing was repeated at 1000  $\mu\text{m}$  along  $x$  and  $y$ -axes. We can easily drive the load difference  $\Delta L_1$ ,  $\Delta L_2$  at maximum depth from the indentation load-depth curves. The conversion factor ratio is already determined from experiments, so from Eq. 2-6, we can evaluate the stress ratio and compare it with the actual one.

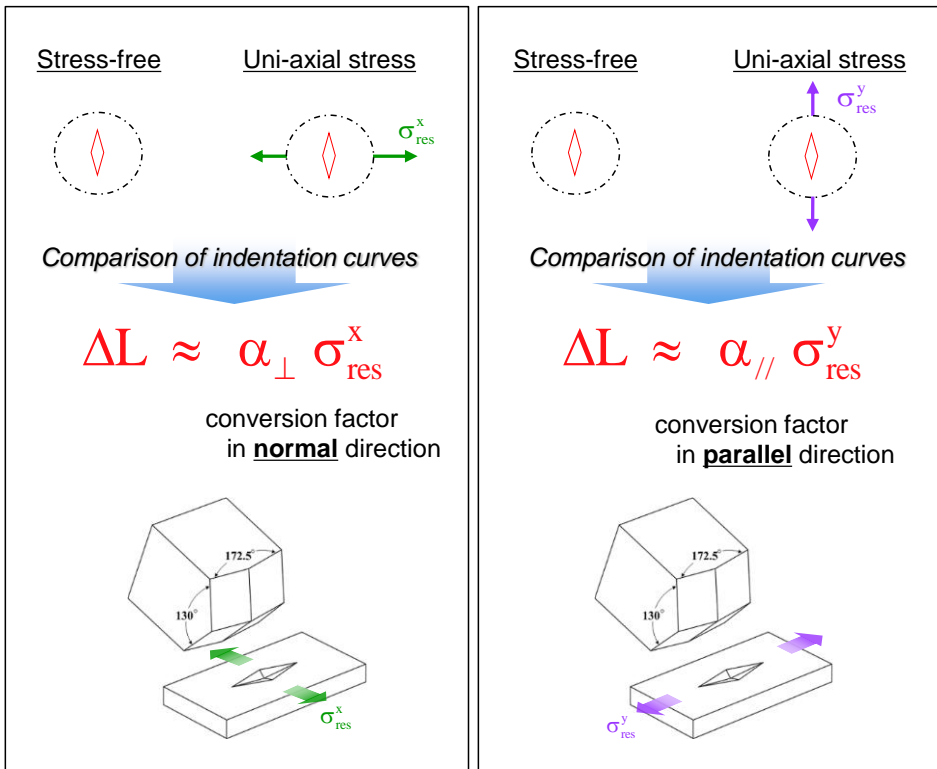


**Figure 4.1** Definitions of conversion factors

<b>Materials</b>	<b>Elastic Modulus (GPa)</b>	<b>Yield Strength (MPa)</b>	<b>Applied Stress (MPa)</b>	<b>Indentation Depth (nm)</b>
CuC1100	115.0	345.0	134, 240, 330	200, 400, 600, 800, 1000
SUS316	203.6	290.0	169, 219, 280	200, 400, 600, 800, 1000
SUS304	189.9	321.0	125, 186, 207	300, 500, 700, 900
S45C	190.0	343.8	246, 298, 330	300, 500, 700, 900
Al6061	68.9	292.5	165, 213, 286	300, 500, 700, 900

**Table 4.1** Materials` mechanical properties and experimental conditions

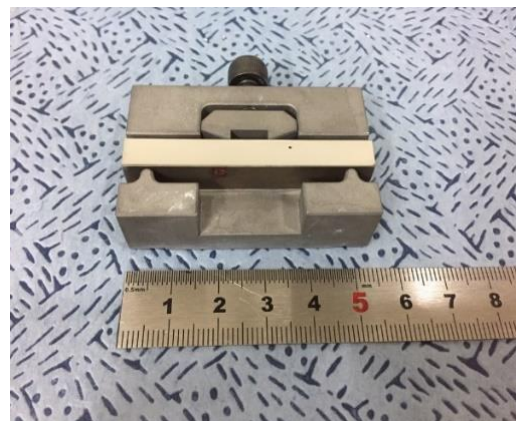


**Figure 4.2** Four-point bending jig

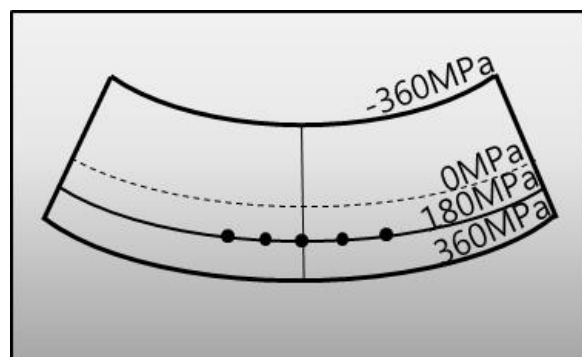


**Figure 4.3** Example of stress distribution of bending specimen



**Figure 4.4** Modified Berkovitch indenter made by PROBES

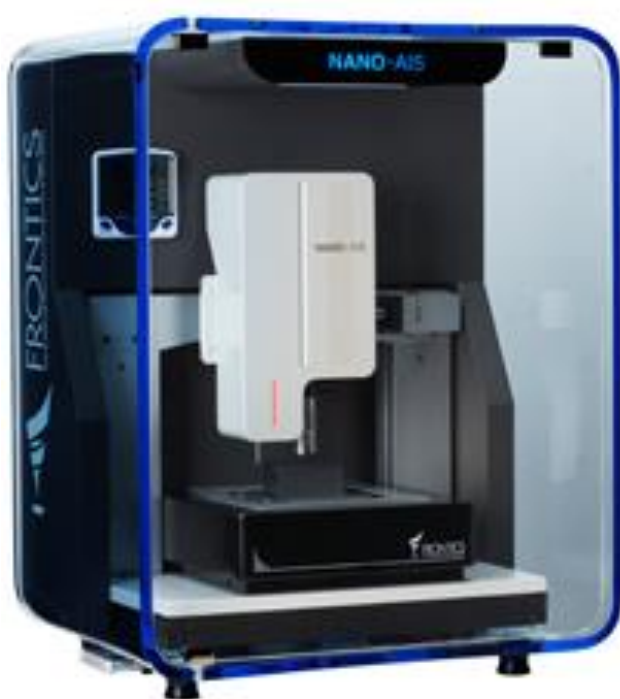


**Fig. 4.5** Nano AIS made by Frontics Inc., Korea



**Figure 4.6** Nano indentation machine made by Anton Paar

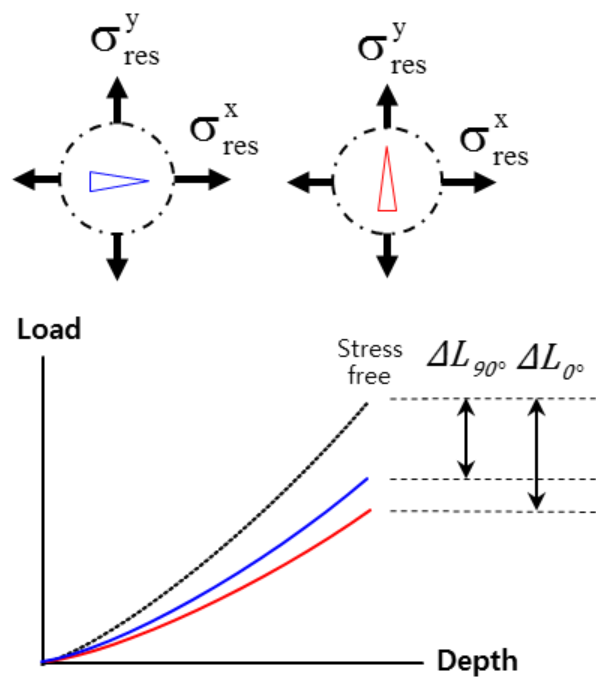


**Figure 4.7** Load-depth curves from different direction of indentations

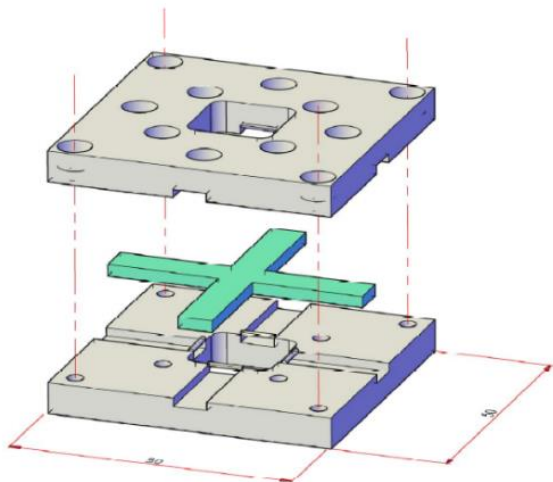


**Figure 4.8** Biaxial stress applied jig and cruciform

Materials	Applied stress (MPa)		Applied stress ratio
	y-axis	x-axis	
CuC1100	232.5	226.0	1.029
Al6061	286.5	81.5	0.325
SUS316	129.0	233.7	0.552
SUS304	176.4	51.8	3.405
S45C	346.2	162.1	2.136

**Table 4.2** Magnitude of applied stresses

## Chapter 5. Results and Discussion

### 5.1 Determination of Conversion Factor Ratio

In order to determine the conversion factor ratio, we use the conversion factor from Eq. 4-1. The conversion factors  $\alpha_{\perp}$ ,  $\alpha_{\parallel}$  are parameters linking the load difference and the applied stress, when specimen is in a uniaxial stress state. Fig. 5.1 ~ Fig. 5.4 show that the conversion factor is the slope of load difference-applied stress curve at a fixed indentation depth,. Using the conversion factors from different indentation depths, we plotted depth (*x-axis*) against conversion factor ratio (*y-axis*), as shown in Fig. 5.5.

As the indentation depth increase, both the nominal conversion factor and parallel conversion factor increase as well. When the conversion factor ratio is fitted to the depth data, as we expected, the conversion factor ratio remains constant at 0.562 regardless of indentation depth, and error range is almost within  $\pm 15\%$  (Fig. 5.5).

## 5.2 Comparison of Measured Stress Ratio with Applied Stress Ratio

In order to compare the measured stress ratio and the applied stress ratio, we apply equibiaxial stress and non-equibiaxial stress to five materials, as shown in Table 5.1. Because the conversion factor ratio is 0.562 regardless of indentation depth, we can derive the stress ratio from

$$p = \frac{\sigma_{res}^y}{\sigma_{res}^x} = \frac{\frac{\Delta L_2}{\Delta L_1} - 0.562}{1 - 0.562 \frac{\Delta L_2}{\Delta L_1}} \quad (5-1)$$

Fig. 5.6 shows the results of comparison of measured stress ratio with applied stress ratio. The error is near  $\pm 20\%$ . We believe that this 20% error may result from the assumption that the load difference in the biaxial stressed state is the algebraic sum of the two load differences in the uniaxial stressed state.

### **5.3 Evaluation of Biaxial Residual Stress using Modified Berkovich Indenter and Berkovich Indenter**

In order to evaluate biaxial residual stress, we first applied stresses as shown in Table 5.2. The sum of the biaxial residual stress can be easily calculated. After measuring stress-free specimen and stressed specimen using Modified Berkovich indenter and Berkovich indenter, the measured ratio and summation of measured stresses were calculated from Eq. 2-4 and Eq. 2-6. We plot the applied stresses and measured stress in Fig. 5.7.

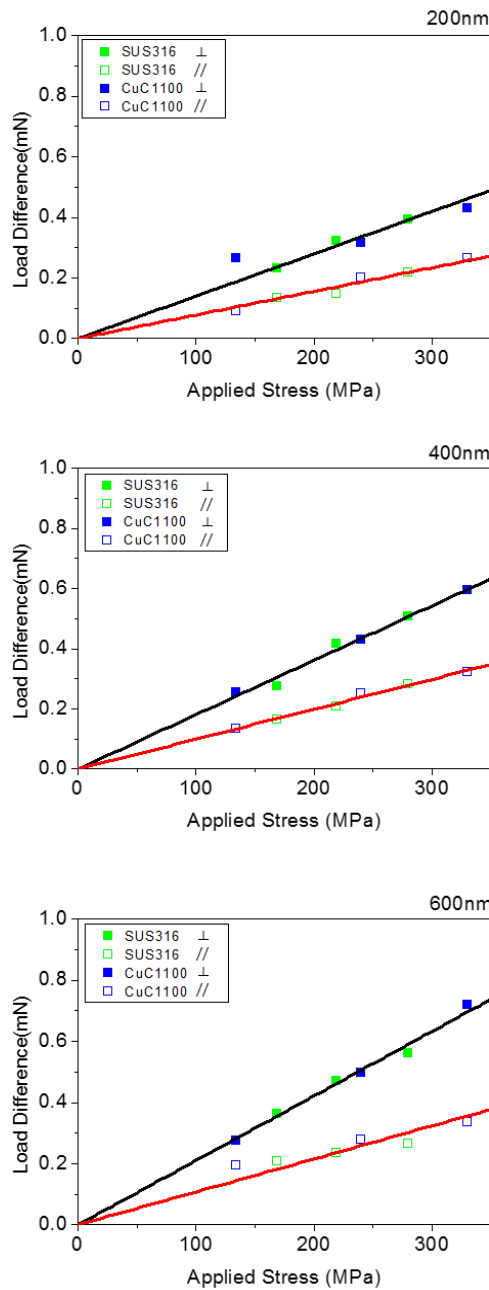


**Figure 5.1** Results of conversion factor ratios

at different indentation depth (1)

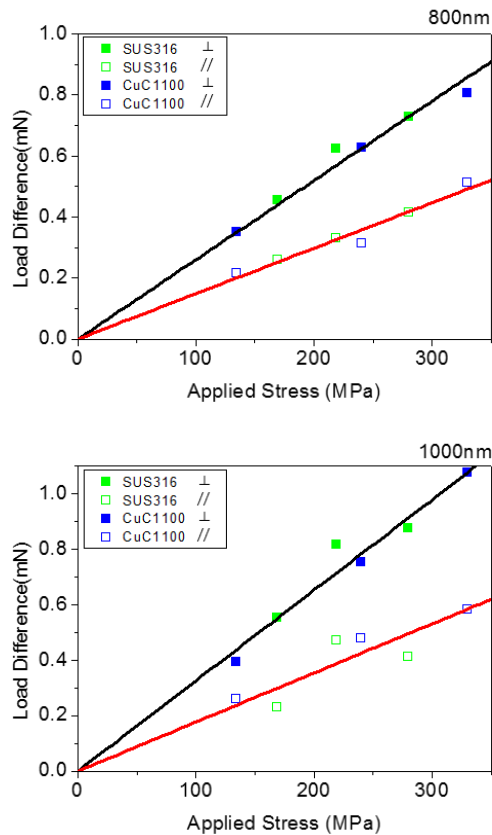


**Figure 5.2** Results of conversion factor ratios

at different indentation depth (2)

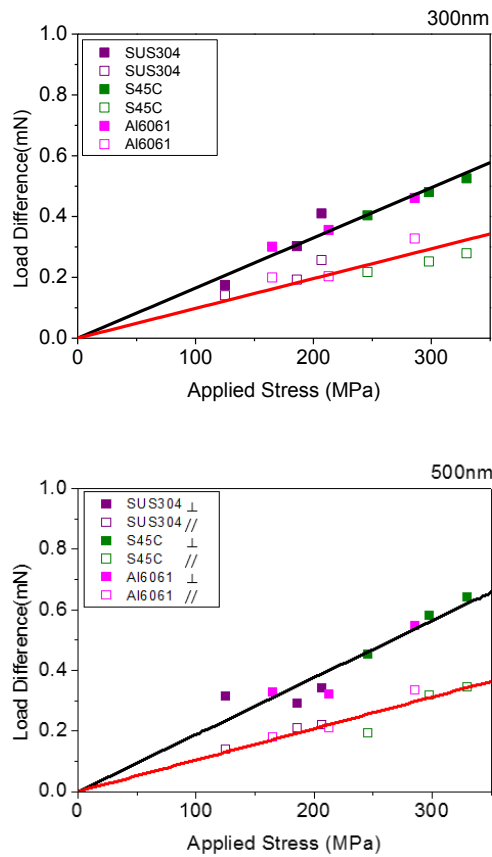


**Figure 5.3** Results of conversion factor ratios

at different indentation depth (3)

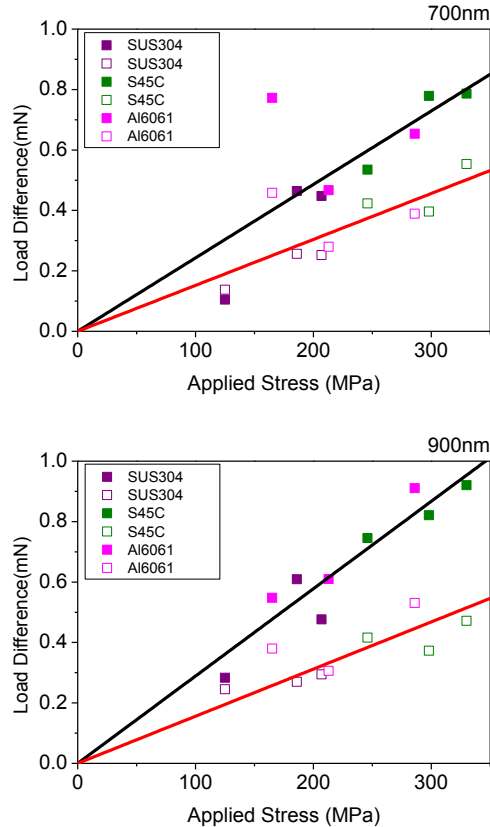


**Figure 5.4** Results of conversion factor ratios

at different indentation depth (4)

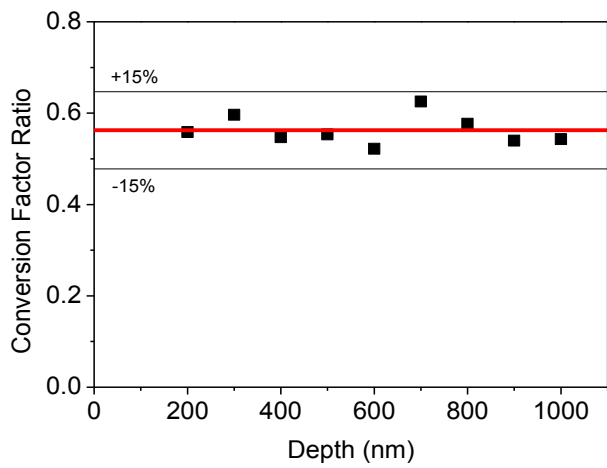


**Figure 5.5** Conversion factor ratios at various indentation depth

Materials	Applied stress (MPa)		Applied stress ratio	Measured stress ratio
CuC1100	y-axis	232.5	1.029	0.874
	x-axis	226.0		
Al6061	y-axis	86.1	0.325	0.382
	x-axis	264.8		
SUS316	y-axis	129.0	0.552	0.492
	x-axis	233.7		
SUS304	y-axis	176.4	3.405	2.892
	x-axis	51.8		
S45C	y-axis	346.2	2.136	1.980
	x-axis	162.1		

**Table 5.1** Applied stress ratios and measured stress ratios

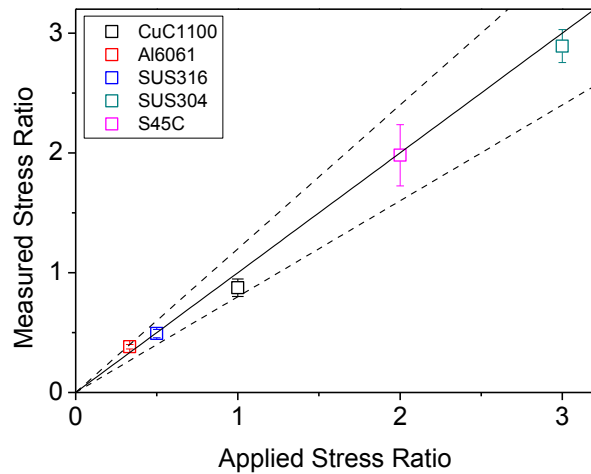


**Figure 5.6** Results of measured stress ratio and applied stress ratio

materials	applied stresses (MPa)			$p$	measured stresses (MPa)		
	$\sigma_{\text{res}}^x$	$\sigma_{\text{res}}^y$	$\sigma_{\text{res}}^x + \sigma_{\text{res}}^y$		$\sigma_{\text{res}}^x$	$\sigma_{\text{res}}^y$	
CuC1100	226.0	232.5	458.5	0.874	406	216.6	189.4
Al6061	264.8	86.1	350.9	0.382	346.7	250.9	95.8
SUS316	233.7	129.0	368.0	0.492	379.6	254.4	125.2

**Table 5.2** The value of applied stresses and measured stresses

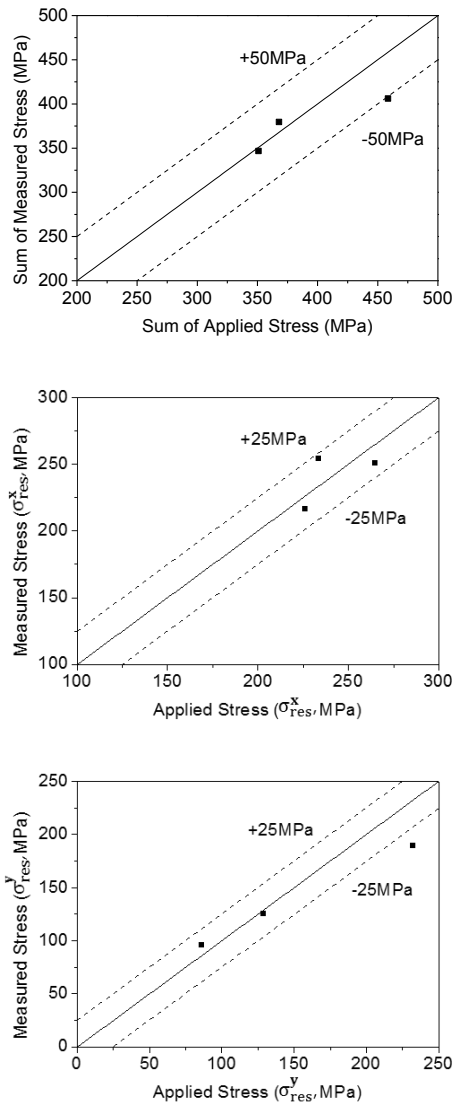


**Figure 5.7** Comparison of applied stress and measured stress

## **Chapter 6. Conclusion**

1. The Modified Berkovich indenter was designed to evaluate biaxial residual stress using instrumented indentation test on nanoscale. This new indenter was modified from a Berkovich indenter that has geometrical self-similarity.
2. Using the Modified Berkovich indenter, we measured normal and parallel conversion factors in the unstressed and stressed states. As expected, the conversion factor ratio remained constant at 0.562 due to the indenter's geometrical self-similarity.
3. Cruciform specimens were chosen to apply the biaxial stress to specimen. The error between the measured stress ratio and applied stress ratio is 20%.
4. Biaxial residual stresses are measured and compared to applied stresses. The error range is  $\pm 25\text{ MPa}$ .

## References

- [1] Weili Cheng, Iain Finnie: *Residual Stress Measurement and the Slitting Method* (Springer US, 2007)
- [2] S. Suresh, A.E. Giannakopoulos, *Acta Mater.* **46**, 5755 (1998).
- [3] Y.-H. Lee, D. Kwon, *Scripta Mater.* **49**, 459 (2003).
- [4] Y.-H. Lee, D. Kwon, *Acta Mater.* **52**, 1555 (2004).
- [5] J.H. Han, J.-S. Lee, M.-J. Choi, G. Lee, K.-H. Kim, D. Kwon *Key Engineering.* 345, 1125 (2007)
- [6] F. Knoop, C.G. Peters, W.B. Emerson, *J. Res. Natl. Bur. Stand.* **23**, 39 (1939).
- [7] M.E. Stevenson, M. Kaji, R.C. Bradt, *J. Eur. Ceram. Soc.* **22**, 1137 (2002).
- [8] F. Ebrahimi, A. Gomez, T.G. Hicks, *Scripta Mater.* **34**, 337 (1996).
- [9] K. Zeng, A.E. Giannakopoulos, D. Rowcliffe, P. Meier, *J. Am. Ceram. Soc.* **81**, 689 (1998).
- [10] G.U. Oppel, *Exp. Mech.* **4**, 135 (1964).
- [11] P.J. Blau, *Scr. Metal.* **14**, 719 (1980).
- [12] Th. Zisis, A.E. Giannakopoulos, *Int. J Solids Struc.* **48**, 3217 (2011).
- [13] A.E. Giannakopoulos, Th. Zisis, *Mech. Mater.* **57**, 53, (2013).

- [14] J. Li, C. Ding, *Surf. Coat. Tech.* **135**, 229 (2001).
- [15] E. Amitay-Sadovsky, H.D. Wagner, *Polymer* **39**, 2387 (1998).
- [16] M.L. Weaver, M.E. Stevenson, R.C. Bradt, *Mat. Sci. Eng. A* **345** 25, 113 (2003).
- [17] A.E. Giannakopoulos, Th. Zisis, *Int. J Solids Struc.* **48**, 175 (2011).
- [18] S. Mukerji, T. Kar, *Mater. Res. Bull.* **35**, 711 (2000).
- [19] J. Borc, *Materials Chemistry and Physics* **137**, 617 (2012).
- [20] P.E. Riches, N.M. Everitt, D.S. McNally, *J. Biomech.* **33**, 1551 (2000).
- [21] P.E. Riches, N.M. Everitt, A.R. Heggie, D.S. McNally, *J. Biomech.* **30**, 1059 (1997)
- [22] E.K Girija, G.R Sivakumar, S Narayana Kalkura, P Ramasamy, D.R Joshi, P.B Sivaraman, *Mat. Chem. Phys.* **63**, 50 (2000).
- [23] M.-J. Choi, S.-K. Kang, I. Kang, D. Kwon *J. Mater. Res.* **27** 121 (2011).
- [24] W.D. Nix, *Metall. Mater. Trans. A* **20**, 2217 (1989).
- [25] L.B. Freund, S. Suresh: *Thin Film Materials: Stress, Defect Formation, and Surface Evolution* (Cambridge University Press, Cambridge, 2003).
- [26] W.D. Nix, B.M. Clemens, *J. Mater. Res.* **14**, 3467 (1999).
- [27] G. Sines, R. Carlson, *ASTM Bulletin*, February, **180** 35 (1952).
- [28] J. Frankel, A. Abbate, W. Scholz, *Exp. Mech.* **33**, 164 (1993).
- [29] T.Y. Tsui, W.C. Oliver and G.M. Pharr, *J. Mater. Res.* **11** 752 (1996).

## 초 록

잔류응력은 주로 재료의 가공 과정이나 열화학적 처리를 받을 때 많이 발생되는데 이런 잔류응력은 실제 인가되는 외부응력과 결합하여 재료의 변형 및 파괴특성에 영향을 준다. 압연공정을 거친 박막소재는 비등방 이축 잔류응력이 걸려있게 되는데 이는 소재의 신뢰성을 현저히 떨어뜨린다. 기존에 잔류응력을 평가하는 선회절법이나 곡률법은 미세조직에 대한 요구가 높거나 표면 평균 잔류응력 평가만 가능한 단점이 존재한다. 하지만 연속압입시험법은 비파괴적인 측정법으로 간편하고 정량적으로 국부 잔류응력을 평가할 수 있는 우세가 있다.

매크로 스케일에서는 Vickers 압입자를 활용하여 잔류응력의 크기를 평가하고 Knoop 압입자를 활용하여 잔류응력의 이방성을 평가한다. 나노 스케일에서는 Berkovich 압입자를 사용하여 잔류응력 크기를 평가한다. 하지만 나노 스케일에서 연속압입시험법으로 잔류응력의 주응력 비를 평가하는 연구는 진행되어온 바가 없다.

본 연구에서는 나노 스케일에서의 이축 잔류응력을 평가하기 위하여 기존의 Berkovich 압입자를 한 방향으로 연장하여 같은 응력 상황에서 같은 압입깊이로 압입하였을 때 하중을 다르게 감지할 수 있는 Modified Berkovich 압입자를 설계 및 제작하였다. 제작 전 유한요소해석을 통하여 새로운 압입자의 유효성을 검증하였다. 기

학적 자기유사성을 갖고 있는 Modified Berkovich 압입자를 사용하여 다른 압입깊이에서 여러번의 일축 응력을 인가하고 응력환산 계수를 측정하였다. 십자시편에 대하여 다양한 잔류응력을 인가하고 Modified Berkovich 압입자를 압입방향을 바꿔가면서 실험을 수행하여 압입하중-변위 곡선으로부터 이축 잔류응력의 주응력 비를 평가하였다. 실제 인가한 응력과 평가된 응력의 비교로 부터 잔류응력의 평가 모델을 검증하였다.

**주요어:** 계장화 압입시험법, **Modified Berkovich** 압입자, 잔류응력, 주응력비, 응력환산계수

**학번:** 2015-22133